ASSESSMENT OF EEG EVENT-RELATED DESYNCHRONIZATION IN STROKE SURVIVORS PERFORMING SHOULDER-ELBOW MOVEMENTS

by

MICHAEL FU

Submitted in partial fulfillment of the requirements

for the degree of Master of Science

Thesis Advisors:

Dr. M. Cenk Çavuşoğlu

Dr. Janis J. Daly

Department of Electrical Engineering and Computer Science

CASE WESTERN RESERVE UNIVERSITY

January, 2006

Contents

List of Tables

List of Figures

Abbreviations

ALS - Amyotrophic Lateral Sclerosis

ANOVA - Analysis of Variance

BCI - Brain-Computer Interface

CAR - Common Average Reference

CD - Complex Demodulation

EEG - Electroencephalography

EMG - Electromyography

ERBP - Event-Related Band Power

ERD - Event-Related Desynchronization

FbEEG - Full-Band Electroencephalography

MRCP - Movement-Related Cortical Potential

SCI - Spinal Chord Injury

SNR - Signal-to-Noise Ratio

Assessment of Event-Related Desynchronization in Stroke Survivors Performing Shoulder-Elbow Movements

Abstract

by

MICHAEL FU

It is unknown whether electroencephalography (EEG) signal characteristics in stroke survivors with motor deficits register enough activity for use with brain-computer interfaces (BCIs). This research studied pre-movement EEG from shoulder-elbow movement in stroke survivors to identify signal characteristics potentially useful for robot-assisted stroke rehabilitation. Pre-movement event-related desynchronization (ERD) was examined in the alpha band mu rhythm for control (n =7) and stroke subjects (n = 11). Subjects were all right-hand dominant; stroke subjects used their afflicted arm and controls were assigned a side to match stroke subjects. Both non-dominant-arm-tested stroke and control subjects exhibited greater ERD intensity vs. those using their dominant arm ($p < 0.05$). Also, pre-movement ERD was detected in stroke survivors, which suggests at the possibility of using ERD as a BCI system control signal. However, the peak ERD of stroke survivors was significantly lower than that of healthy subjects ($p < 0.05$), which brings doubt to whether the intensity of ERD in stroke survivors is large enough to be used as a BCI system control signal.

Chapter 1

Introduction

Cortical activity driving motor-related activity has become an important field of research for studies attempting to decode the brain's electrical activity for use as a control signal in brain-computer interfaces (BCIs) or brain-machine interfaces (BMIs). Many studies reported use of BCI or BMI to improve the lives of people suffering from spinal chord injuries (SCI) or amyotrophic lateral sclerosis (ALS) [7]. Patients with SCI or ALS can plan out or imagine movements normally, but not perform them. In these studies, the brain's neural activity was detected during imagined movements and translated into prosthesis control signals or into mouse cursor motions for communication purposes.

Cortical activity as a result of motor-related planning exists not only in normal, undamaged brains, but also in the brains of stroke survivors, despite the injury that ischemia inflicts in the brain [8]. However, because of the ischemia, damaged neurons, and potentially altered neural activity, it is unknown whether EEG in stroke survivors can be used in BCI. The purpose of this research study was to characterize EEG in stroke survivors in order to identify signal characteristics that could potentially be used in BCI applications.

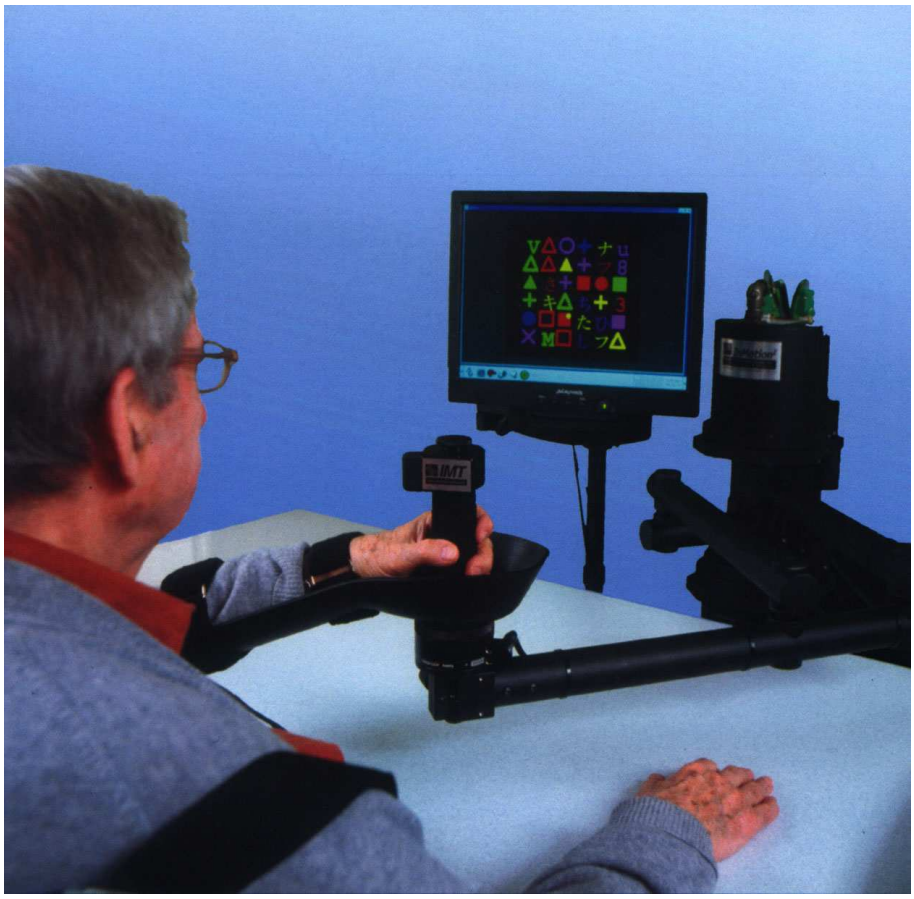

Figure 1.1: The Inmotion^2 Shoulder-Elbow Robot is used in upper extremity physical rehabilitation therapies and only allows 2D shoulder-elbow movements [1].

1.1 Thesis Contributions

The objective of this thesis was to extend existing literature in a number of ways. First, the event-related desynchronization characteristics of stroke-affected EEG during a shoulder-elbow motion were evaluated during use of the Interactive Motion Technologies, Inc. (Cambridge, MA) Inmotion^2 Shoulder-Elbow Robot (Fig. 1.1). Second, new information was identified regarding EEG signal characteristics for dominant versus non-dominant shoulder elbow movements for both healthy controls and stroke survivors.

1.2 Thesis Outline

The remainder of this thesis is organized as follows. Several relevant background topics and existing research are discussed in the Background (ch. 2) and Literature Review (ch. 3) chapters. Then, the Methods chapter (ch. 4) describes the experiment paradigm and data analysis techniques that were employed. Findings from this study are reported in the Results chapter (ch. 5) and extensions to literature and study limitations are mentioned in the Discussion chapter (ch. 6). Key findings and further research directions are also described in the Discussion chapter.

Chapter 2

Background

This section will discuss information and current research regarding stroke, EEG waves, and BCI. Niedermeyer and Lopes da Silva's text *Electroencephalography* [9] and Bogousslaysky and Caplan's text *Stroke Syndromes* [10] are definitive texts on EEG and stroke, respectively.

2.1 Background on Stroke-related Motor Deficits

A stroke occurs when a blood vessel leading directly to the brain can no longer deliver oxygen and nutrients to it, resulting in the death of cortical tissue. There are two types of stroke: 1) an ischemic stroke occurs when a blood clot blocks blood from entering the brain and 2) a hemorrhagic stroke occurs when a blood vessel ruptures. In a normal adult, motor tasks on a particular side of the body are controlled by the side of the brain contralateral to the side of motion (for instance, a right arm movement is controlled by the left side of the brain). Therefore, if a stroke occurs near the sensory or motor areas of the brain (Fig. 2.1) various motor deficits can occur and impair the side of the body contralateral to the damaged side of the brain.

Some of the motor impairments that can occur are hemiparesis, hemiplegia and motor aphasia. Hemiparesis is a weakness in the muscles of a single side of the

body, whereas hemiplegia is a total paralysis of one side of the body. Stroke victims suffering motor aphasia, on the other hand, might have little trouble with executing movements, but are unable to understand how objects are used. For instance, they will see a hammer and a nail and not understand how to use the hammer on the nail. The stroke survivors in this study suffered from hemiparesis or hemiplegia.

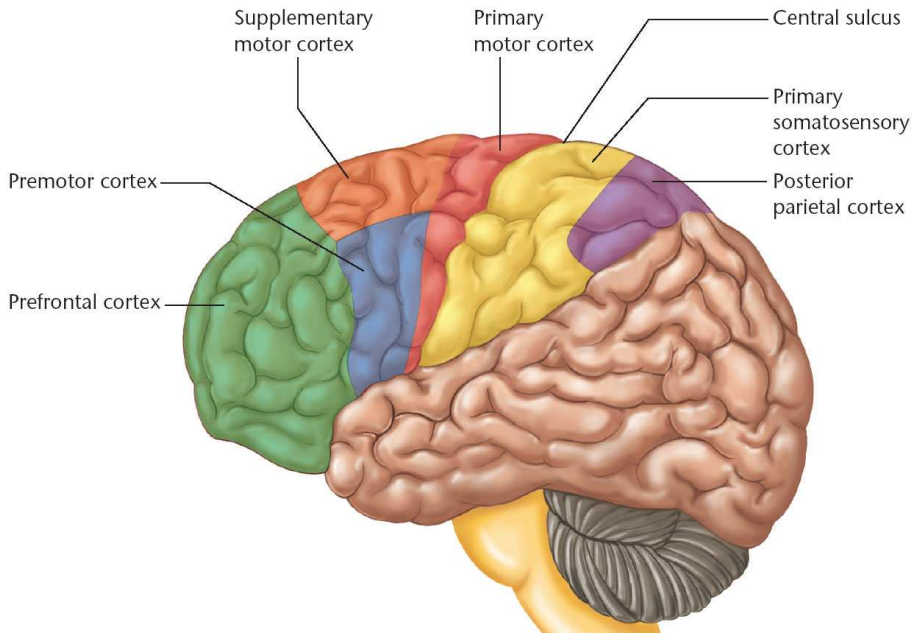

Figure 2.1: The major cortical regions of the brain over which EEG electrodes were placed [2].

2.2 Background on EEG

Electroencephalography (EEG) signals are recorded in terms of voltage (microvolts in scale) by electrodes placed on the scalp of a subject and were first studied by Hans Berger in humans in 1920 [9]. The recorded signals result from fluctuating extracellular electric field potentials surrounding neurons in the brain. When active excitatory or inhibitory synapses alter the electric signal arriving from the neuron, the result is a fluctuating field potential that can be measured at the scalp with electrodes and amplifiers. The current standard for electrode placement is the International 10-

20 system (Figure 2.2). Each electrode is 8 mm in diameter and has a cavity depth of 5 mm in which conductive gel can be injected to lower impedance between the electrode and the scalp. The electrodes are labeled by their location on the scalp (F for frontal, C for central, T for temporal, P for parietal, and O for occipital) and numbered so that the Z (for zero) electrodes run down the center, odd electrodes are on the left hemisphere, and even electrodes are on the right.

Prior to practical analog to digital conversion technologies, EEG recordings were plotted onto paper and visually examined. But since the 1970s, the norm has become frequency domain and statistical analysis of EEG signals with computers. Like other bioelectric signals, EEG waves are quasi-periodic, but for analysis purposes several frequency band classifications of EEG have been defined by researchers and are named in the order of their discovery — not by their order in the frequency spectrum. Five commonly studied ones are: alpha band (8–13 Hz), beta band (14–30 Hz), gamma band (30–70 Hz), delta band (0.1–3.5 Hz), and theta band (4–7.5 Hz) [9].

2.3 EEG Alpha Band

This study focused on EEG signal characteristics in the alpha band. The alpha band was one of the earliest identified by Berger and includes waves oscillating from 8–13 Hz. An increase in the amplitude of alpha waves is best correlated with relaxed wakefulness for the normal adult. Most notably, amplitudes can be enhanced when the eyes are closed (such as during meditation). Typical amplitudes of alpha waves are difficult to define because they vary greatly from person to person, but a typical range can be from 0–50 uV. Values above 100 uV are uncommon in normal adults [9]. Attenuation of the alpha waves, which is also called desynchronization, occurs when the subject is either attentive, anxious, or in a state of expectancy to external stimuli. Therefore, motor task planning attenuates waves in this frequency band.

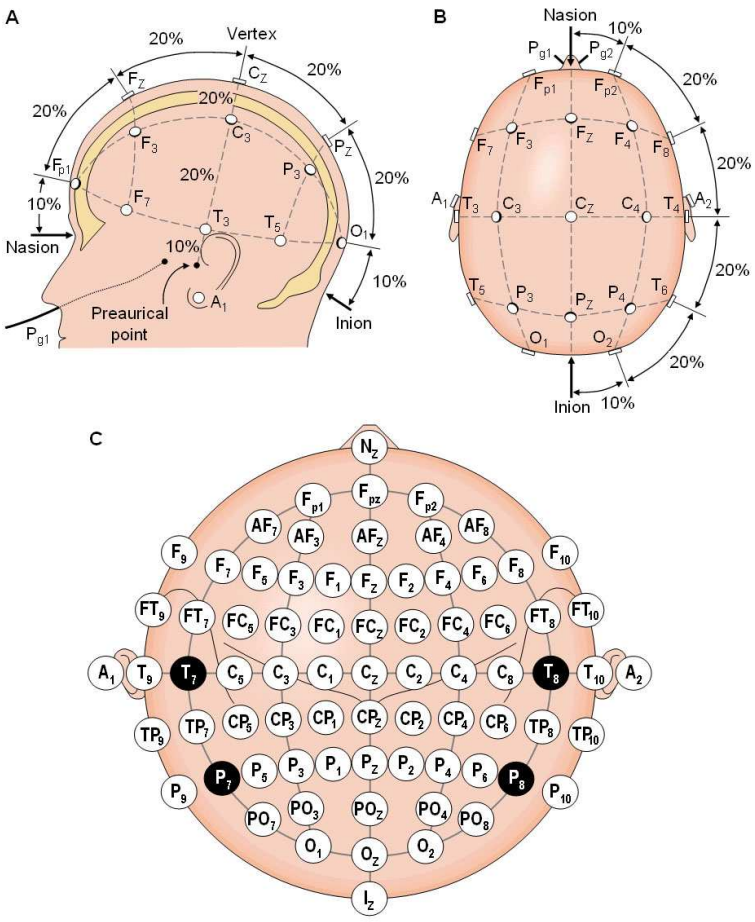

Figure 2.2: Different perspectives of the International 10-20 standard system of electrode placement. (A) Sagittal plane, (B) axial plane, and (C) the locations of the 64 electrode configuration used in this study [3].

2.4 Mu or Rolandic Waves

Mu waves, also known as Rolandic waves, were discovered by Jasper and Andrews in 1938 and are known to exist in the alpha band. Mu stands for motor and in most healthy adults, the mu wave is attenuated whenever movements (voluntary, passive, or reflexive) are performed or even imagined. Mu wave attenuation occurs up to, and sometimes beyond, 2 s before movement onset. It has key, harmonically unrelated frequency components at around 10 Hz (alphoid component) and at 20 Hz (beta component). The alphoid component can exist anywhere from 8 Hz to above 11 Hz in some adults. The alphoid component of the mu wave arises from the somatosensory

cortex (Fig. 2.1), so it is usually most active and detectable under the CP EEG electrodes that overlay the parietal area, which can be seen by comparing Figure 2.1 with Figure 2.2A. The beta component of the mu wave, however, arises from the motor cortex (Fig. 2.1) and is most active under the CZ, C3, and C4 electrodes (Fig. 2.2C). Both the alpha and beta band mu components exhibit attenuation, or desynchronization, prior to and during movements [11].

2.5 Event-Related Desynchronization

Brain activity during sensory processing or motor behavior was first reported by Berger in 1930 and can be observed in EEG data as the desynchronization, or attenuation, of alpha and beta band waves. Event-related desynchronization (ERD) refers to desynchronization that occurs due to voluntary or involuntary activity. It is also a reliable correlate of increased cellular excitability in the thalamocortical systems during cortical information processing [9]. In contrast, when the brain is idling (at rest), alpha waves are enhanced, reflecting greater amplitudes in the EEG data. One theory on the cause of desynchronization is that neurons behave like weakly-coupled non-linear oscillators which synchronize with each other when the brain is idle, but desynchronize from the weak coupling when processes become active in the brain [12].

Gert Pfurtscheller developed the ERD percentage measure to quantify the amount of EEG desynchronization, [9]. The measure is formally defined as

$$ERD\%_{decrease} = 100 \times \frac{Power_{ref} - Power_x}{Power_{ref}} \tag{2.1}$$

where $Power_{ref}$ is the average power in a reference interval (typically a period of time that is a few seconds while the subject is at rest) and $Power_x$ is the average power in an interval of interest with which we wish to compare the reference interval for activity in the EEG data. A positive ERD percentage indicates that there is a

decrease in power with respect to the reference state and a negative value means there is an increase in power.

In ERD analysis of motor tasks, the subject is asked to perform multiple trials of the task so that the mu wave can be identified. This is accomplished by identifying the frequency in the alpha and beta bands, for which there is a maximum difference in average power between the rest and motor-planning states. Then, each trial's time-domain EEG data is bandpass filtered to include only mu frequency signals, squared to obtain power, and finally the ERD percentage equation is applied to the data with $Power_{ref}$ as defined and $Power_x$ as each sample of data in the bandpassed and squared data. Figure 2.3 gives a graphical example of the calculation and the resulting time-series ERD% plot.

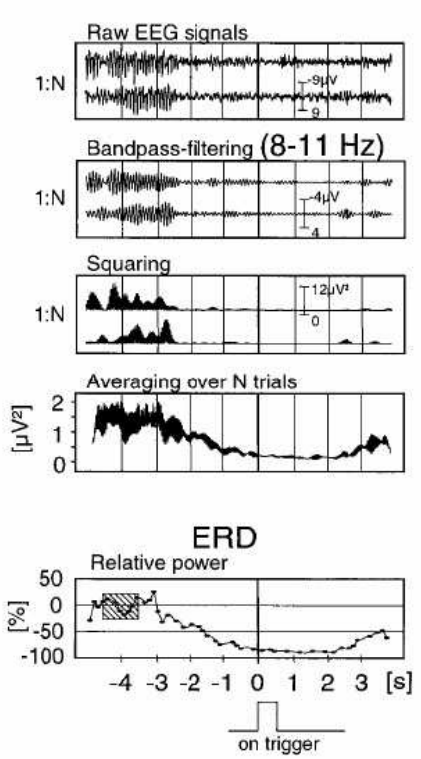

Figure 2.3: An illustration of an ERD% calculation and the resulting time-domain plot [4].

2.6 Movement-related Cortical Potential

ERD is most noticeable in the 8–12 Hz range, but there is also a movement-related EEG activity in the slow, 0.1–1 Hz range called the movement-related cortical potential (MRCP). MRCPs are negative potentials that can be seen in the raw EEG data after averaging many trials of the same motor task together (Fig. 2.4). The initiation of the MRCP curve occurs before movement onset and is the beginning of pre-motor planning [9]. The amplitude of the curve is correlated with the amount of cognitive effort. For example, one would suspect that using the non-dominant hand to perform a motor task requires more focus or effort, which should be detectable in the MRCP. And in fact, Tarkka found that the MRCP for moving the non-dominant index finger starts earlier and rises to higher amplitude than dominant finger movements [13]. Although the MRCP reflects cortical activity, it is not practical as a BCI input signal because it is discernable only after averaging many trials, unlike ERD. MRCP and ERD share common timing characteristics, though, so MRCP start times and duration can be used to help identify periods of cortical activity in which ERD should be present [14].

2.7 Brain Computer Interface

BCI systems are designed to translate the brain's activity during imagined movements into computer cursor or prosthesis control. Wolpaw, *et al.* at the Wadsworth Center for Laboratories and Research in NY implemented a pioneering EEG-based BCI system in 1991 [15]. This system measured the amplitude of mu waves to allow a well trained subject to control the direction of a cursor in one dimension by varying the amplitude of their mu waves [15]. In 2004, the same group was able to make two dimensional control possible using noninvasive EEG, even though it was widely assumed that only invasive recordings of brain waves can provide the resolu-

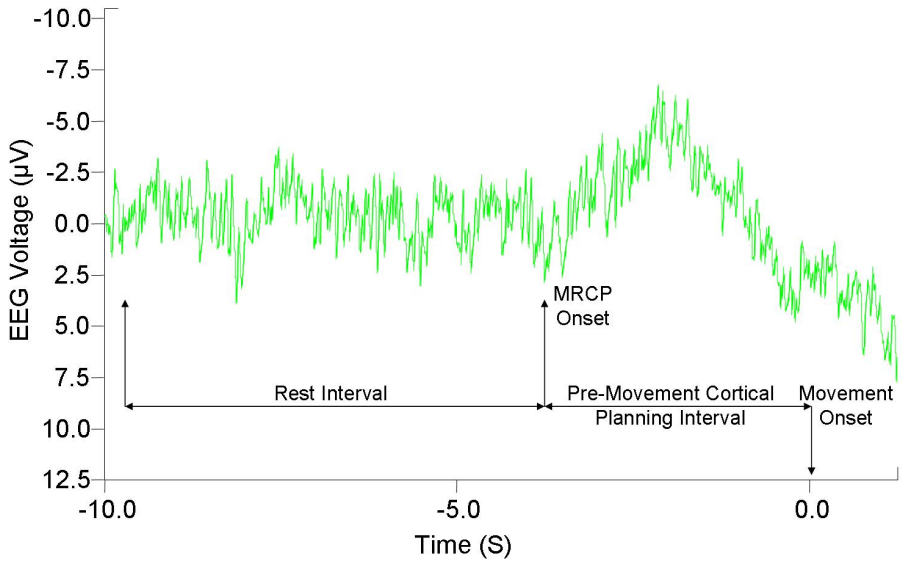

Figure 2.4: Example of an MRCP curve starting from baseline approximately 4 s before movement onset.

tion needed to achieve 2D control [16]. These advancements in noninvasive EEG BCI systems are important for developing a BCI system for stroke survivors because invasive recordings require implanted electrodes under the skull, which is not desirable for individuals who already have stroke-induced damage to their brains.

Stroke survivors are unique from other types of people who can benefit from BCI because they can be rehabilitated to a greater degree than those suffering from SCI or ALS. Therefore, stroke survivors might best use BCI not as a permanent prosthesis-driving technology, but instead as a rehabilitation tool that might provide therapies to focus on and take advantage of the plasticity of the brain to regain motor control.

Plasticity is the brain's ability to reorganize around damaged cortical areas and recover functions for which those areas were responsible. Using EEG recordings, Sterns, *et al.* discovered that increases in task-related coupling between cortical areas may compensate for brain damage after stroke [17]. They also found that some of the increased coupling decreases as patients make a functional recovery. Therefore, if a BCI system is developed to analyze the EEG of stroke survivors, then it can be paired with a rehabilitation robot to tailor-design therapy sessions which promote

plasticity in the brain of the subject.

Since the 1990s, rehabilitation robots have become an effective component of stroke therapy studies [18]. Unlike a self-evoked motion, robots like the Inmotion^2 Shoulder-Elbow Robot (Fig. 1.1) challenge and assist stroke survivors to accomplish movements they cannot otherwise successfully perform. Lum, *et al.* even found that robot-assisted therapy helped stroke survivors improve more (in both biomechanical and Fugl-Meyer assessment of motor impairment measures) than conventional therapy did [19]. A combination of robotic rehabilitation and BCI would allow therapists to actively measure and restore lost motor skills cortically, instead of only functionally. However, there are currently no studies on the effect of stroke on the EEG of subjects executing movements that can be assisted with a rehabilitation robot.

Chapter 3

Literature Review

This section will discuss existing literature regarding two topics relevant to this thesis: 1) EEG characteristics in stroke survivors and 2) the use of EEG as a control signal in stroke rehabilitation.

3.1 EEG Characteristics in Stroke Survivors

EEG signals during motor tasks have been characterized in normal adults. The purpose of the current study was to characterize EEG signal in stroke survivors and determine whether any of the characteristics of the EEG signal would be potentially useful for BCI in stroke survivors with sensorimotor cortex damage. There was some doubt about this issue, as sensorimotor cortical damage might render the cortical signal useless as a control signal or in rehabilitation applications. In fact, Daly, *et al.* found that the initiation of cognitive planning in stroke survivors was significantly delayed versus healthy control subjects ($p < 0.05$) [20]. Daly, *et al.*'s study was the first to report on pre-movement cortical motor planning for a shoulder-elbow motor task. The outcome measure that was used was an averaged "off-line" (not in real time) calculation of motor planning time. In order to use EEG signals "on-line" (in real time) during motor re-training, a characteristic of the raw signal must be

identified. BCI systems currently use mu rhythm ERD as a BCI control signal for normal, ALS, and SCI subjects [15]. The purpose of the current study was to evaluate the usefulness of ERD in order to identify a real-time measure of brain activity.

Most studies of healthy adults focused on ERD during finger movements [8], [21], and [11]. Platz, *et al.* investigated cortical motor planning by using a motor task that involved the index finger tracing a small triangle. Functional movements involve the use of shoulder and elbow movements, and stroke survivors often have impairment in the control of these movements [8]. Therefore, shoulder-elbow movements in stroke survivors were studied. The only study that examined a shoulder-elbow movement was Labyt, *et al.*, who studied the ERD of a targeting movement in which subjects pointed to a target in front of them with their index finger, but the subjects were healthy young and elderly adults [22]. In contrast, the subjects in the current study were not required to be able to complete the movement required for the motor task.

3.2 Evaluation of EEG Characteristics for Stroke Rehabilitation Use

Conventional therapies do not restore normal control to many stroke survivors. Therefore, it is critical to identify more effective stroke rehabilitation strategies. The use of mu wave ERD as a control signal has shown some promise in normal adults, locked in syndrome, ALS, and SCI [15], [7]. BCI users typically train to voluntarily modulate their mu waves by imagining movement and inducing ERD [15]. These changes in signal amplitude are then detected and translated into control signals for communication or prosthetic control [23].

It is not clear whether the EEG signal can be used for stroke survivors as a control signal or in rehabilitation of motor or cognitive function. There is no literature on stroke survivors using BCI and Daly, *et al.*'s discovery that stroke survivors have

delayed cortical planning periods versus healthy controls raises doubts about whether stroke survivor EEG is compatible with BCI systems [20].

This study also investigated whether the effect of hand dominance on the EEG signal characteristics for shoulder-elbow movement is consistent with literature on finger movements. Tarkka studied the healthy adults performing finger movements on different hands and found that the MRCP began significantly earlier and with elevated intensity for subjects moving their non-dominant hand versus dominant-side movements ($p < 0.05$) [13]. Consistent with this finding, Stancak reported an earlier start and greater percentage of ERD for non-dominant finger movements compared with dominant hand movements [24]. Finally, Bai *et al.* provided the most recent findings on this topic in a 2005 study investigating hand dominance using ERD correlated with EMG signals [21]. They reported that, compared to the non-working side of the brain during dominant hand finger movements, there is more activity on the non-working side of the brain when fingers of the non-dominant hand are moved. To date, there is no available information regarding ERD for dominant versus non-dominant upper limb during shoulder or elbow movements for either healthy or stroke subjects.

Another gap in the literature is that there are currently no published studies on the EEG signals of subjects operating rehabilitation robots. Daly's study was the first, to date, to look at EEG signal activity during cognitive pre-movement planning in stroke subjects using a rehabilitation robot, and this thesis extends those findings [20]. This thesis analyzed ERD measures rather than MRCP measures in order to evaluate whether real-time EEG signal characteristics can accurately reflect pre-movement cortical activity.

Chapter 4

Methods

Event-related desynchronization was the EEG signal characteristic analyzed for this study because it is a reliable correlate of increased cortical activity during information processing [9]. Also, the intensity of ERD relative to a cortical rest interval can be computed in real time to reflect the amount of cortical activity that is responsible for motor task planning. This section describes the methods used to analyze ERD in this thesis. The contents include a description of the subjects recruited for the study, the experimental paradigm and data recording methods, and the data analysis techniques that were used (spatial filtering, noise rejection, and computation of ERD).

4.1 Subjects

Twenty right-hand-dominant subjects were selected and gave consent to enroll in this study. This study was conducted according to the Declaration of Helsinki and oversight was provided by the Internal Review Board of the Louis Stokes Cleveland Veterans Affairs Medical Center. Ages ranged from 48–72 years old, with a mean age of 61. Twelve of these subjects had chronic (> than 12 months) arm coordination deficits following stroke and eight subjects were age-matched, healthy individuals.

4.2 Experimental Paradigm

All of the subjects were seated before a computer screen with either their right or left hand gripping the end-effector of an Inmotion^2 Shoulder-Elbow Robot. Control subjects were randomly assigned to use their left or right arm while stroke survivors used the arm suffering coordination deficits. As illustrated in Fig. 4.1, the subjects were then presented with a motor targeting task that required an accurate 14 cm, linear movement in the horizontal plane beginning at the center of the workspace and moving to a target in a direction directly in front of the subject. This motor task required shoulder flexion and elbow extension, which each subject performed fifty times with a two-minute recess between every 10 trials. Not all stroke survivors could accomplish the normal movements required of the motor task, but all of them made their best effort to do so.

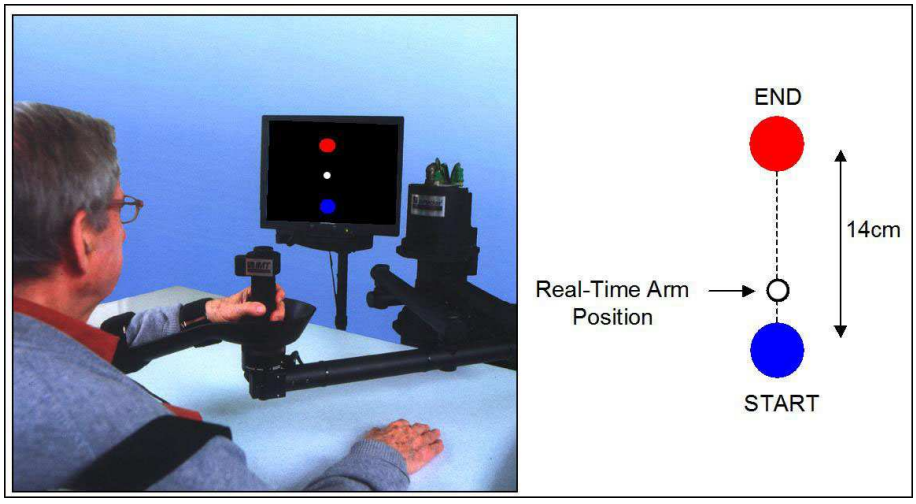

Figure 4.1: Illustration of the experimental paradigm in which the diagram to the right represents what was seen on the subject's screen. The subject was to move from the 'start' circle to stop at the 'end' circle in as straight a line as possible.

4.3 Data Recording

Simultaneous data recordings were obtained for EEG, electromyography (EMG), and movement onset. EEG data were obtained using Compumedics NeuroScan Ltd. (El Paso, TX) devices and software. The data were recorded using NeuroScan Acquire 4.3.1 software, a 64-electrode Quick-Cap EEG cap (Fig. 4.2), and a NeuroScan Synamps amplifier system with a gain of 500, sampling rate of 1000 Hz, and bandpass filter set to pass 0.1–40 Hz (Fig. 4.3). All electrodes on the EEG cap were 8 mm in diameter with a 5 mm cavity depth and were arranged on the scalp in compliance with the International 10-20 standard [25]. Each recording was referenced to the common linked left and right mastoid surface electrodes. All electrode-to-scalp impedances were reduced to less than 10 kΩ using electrically conductive gel and real-time electrode impedance measurements provided by the NeruoScan Acquire software.

Figure 4.2: Photograph of the NeuroScan 64-electrode Quik-Cap used to make EEG recordings in this study.

Figure 4.3: Photograph of the NeuroScan Synamps amplifier system used to make EEG recordings in this study [5].

4.4 Preliminary Data Processing

The EEG data were first examined and filtered for noise. Then, the signal-to-noise ratio (SNR) of the EEG data were optimized by using spatial filtering and searched for any contamination by scalp or facial muscle EMG signals. The locations of greatest brain activity and the corresponding amounts of peak ERD% were identified during pre-movement motor planning.

4.4.1 Noise Rejection

Filtering techniques were applied to the data in order to eliminate noise from the EEG data. The EEG data were first visually inspected by an expert to reject trials containing blink artifacts or abnormalities in the baseline data. Upon further analysis, an unknown noise source with a center frequency at 20 Hz was observed in all of the subjects' data. The noise existed roughly between 19–21 Hz and was non-uniformly distributed across the electrode locations, as seen in Fig. 4.4. To suppress the noise, a 48 dB/octave bandstop filter was applied between 19 and 21 Hz. However, because the

beta band component of mu waves in normal adults are most active at approximately 20 Hz, the noise prevented accurate analysis of the beta band for cortical activity [9]. Therefore analysis was performed only on the alpha band for this study.

4.4.2 Spatial Filtering

Spatial filtering was performed to improve the signal-to-noise (SNR) ratio of the EEG data being analyzed by removing any noise common to all of the electrodes. Using NeuroScan Edit 4.3.1, a common average reference (CAR) was performed on all 64 electrodes in order to produce a 'reference-free' version of the EEG data. CAR was chosen based on its superior SNR characteristics as reported in a study performed by McFarland, which compared several spatial filtering techniques for improving the SNR of EEG signals for BCI use and concluded that the CAR had the best SNR [26]. In the calculation of the CAR, the average value of all 64 electrodes was subtracted from the channel of interest for each sample of data. Specifically, the formula for CAR was

$$V_i^{CAR} = V_i^{ER} - \frac{1}{64}\sum_{j=1}^{64} V_j^{ER} \tag{4.1}$$

where $V_i{}^{ER}$ is the potential between the ith electrode and the reference electrode. The effect of the CAR spatial filter was that any noise common to all the electrodes was reduced from the EEG data.

4.4.3 Scalp EMG Noise Detection and Rejection

EEG recording systems are sensitive to EMG signals produced by the scalp muscles, so any trials affected by EMG signals were removed. Some of the stroke survivors exerted considerable effort while attempting the motor task and there was a possibility that their facial muscles were strained or teeth were clenched. These muscle contractions

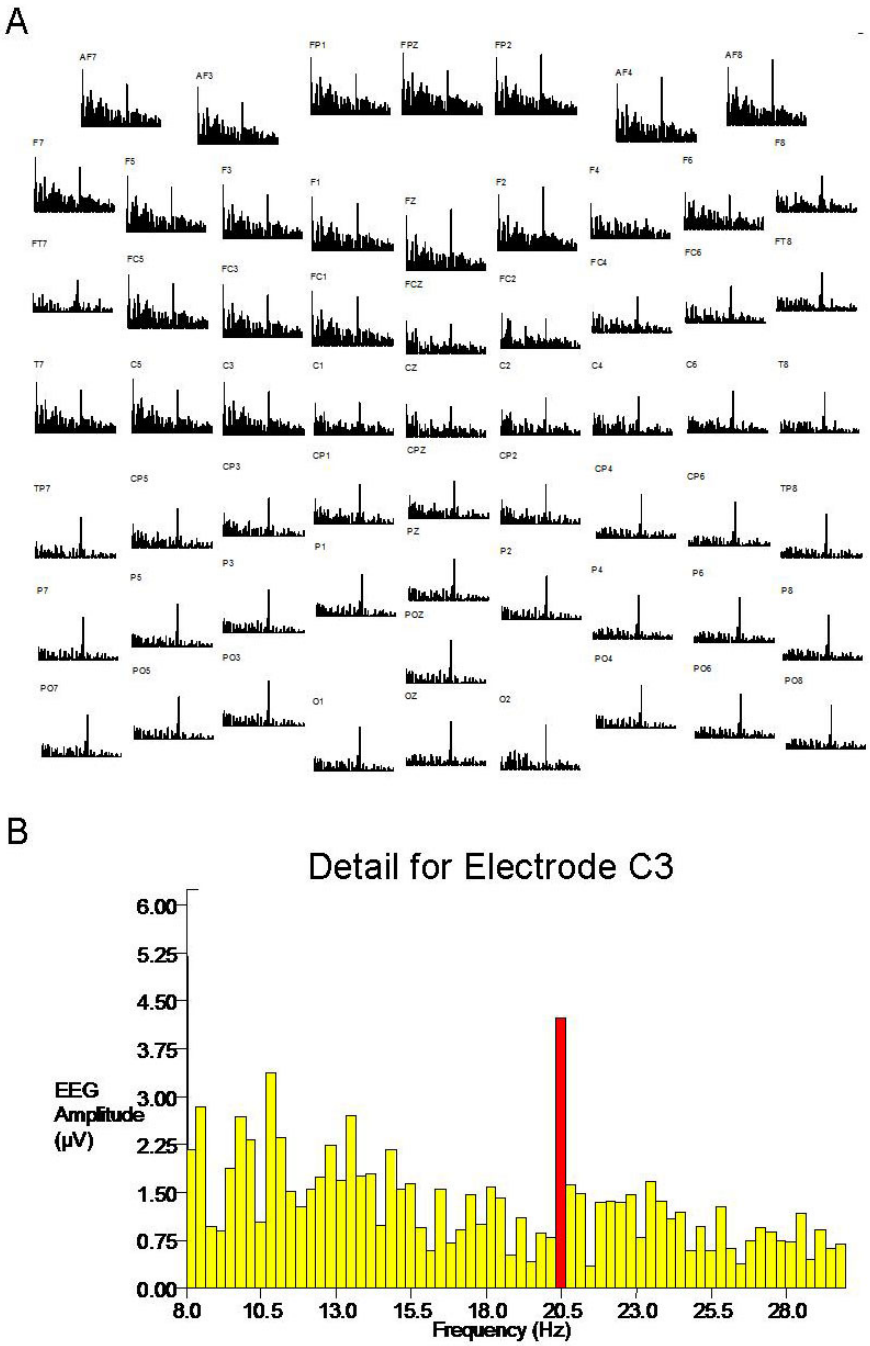

Figure 4.4: A)Frequency-domain plots of the range 8–30 Hz of EEG recordings at 64 electrodes for a randomly selected subject in this study. The vertical axis is magnitude in uV. The effects of the unknown noise source at 20 Hz are clearly visible as the vertical spike in the center of each electrode recording. B) A more detailed plot of electrode C3 reveals that the 20 Hz noise signal (darkened bar) is approximately 4 uV in amplitude and greater than all the other frequency components.

have the potential to introduce EMG activity that could be sensed by the EEG electrodes and subsequently recorded along with cortical activity.

The following methods for EMG detection are largely based on the results of a study by Goncharova on the characteristics of facial and scalp muscle EMG signals as measured through EEG recording equipment [6]. The EMG detection and rejection were performed for both the pre-movement planning interval and the rest interval of each trial, because EMG noise in either interval would have affected the accuracy of ERD calculations. The planning state was defined as the 3 s interval preceding movement onset and the rest state was a separate 3 s interval preceding the planning state. A time interval larger than that used by Goncharova [6] was used since stroke survivors had longer motor planning intervals [20]. The procedures that were followed for the EMG noise detection were consistent in all respects to Goncharova's [6].

EMG from the frontalis and temporalis muscles can be a source of noise when examining EEG signals because the range of frequencies spanned by EEG and EMG overlap. Clinically relevant scalp EEG signals range from 0.1–100 Hz, but EMG ranges from 0 to $>$ 200 Hz [9]. The frontalis muscle (which moves the forehead skin and eyebrows) shows maximum EMG activity from 20–30 Hz and the temporalis muscles (which clench the teeth) have maximum EMG activity from 45–70 Hz. Even with weak contractions, EMG data is detectable at the vertex of the scalp in the 8–12 Hz frequency band (exactly our frequencies of interest), so it was important to reject any trial that might be contaminated with EMG signals from the frontalis or temporalis muscles.

To determine whether a trial contained EMG noise, data were analyzed from four electrode locations that were most susceptible to EMG contamination, which will be referred to as the 'primary' electrodes for EMG rejection, as shown in Fig. 4.5. AF7 and AF8 were most affected by the frontalis muscles, and FT7 and FT8 were most affected by the temporalis muscles. At these electrodes, the 45–70 Hz frequency band

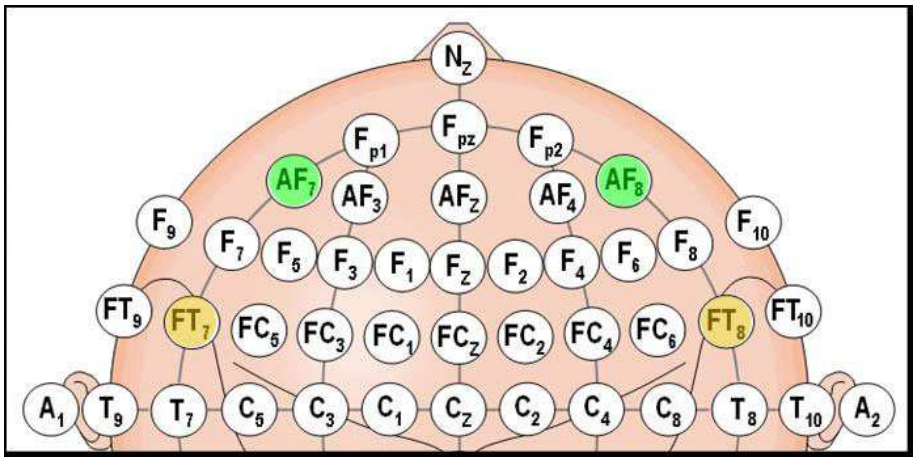

Figure 4.5: Shaded electrodes were the locations where EMG from the scalp muscles showed greatest activity when recorded from EEG electrodes. AF7 and AF8 were affected by the frontalis muscles, while FT7 and FT8 were affected by the temporalis muscles [6].

power was first computed in each trial because scalp muscle EMG exhibits peaks in this frequency band, but EEG signals do not. The power was calculated using the formula

$$Power_{45-70Hz} = \frac{1}{N^2} \sum_{k=\frac{45N}{fs}}^{\frac{70N}{fs}} (|X(k)|^2 + |X(N-k)|^2) \tag{4.2}$$

where N is the total number of samples in the rest or planning state and $X(k)$ is the kth FFT coefficient, and f_s is the sampling frequency.

In any of the 50 trials, if the 45–70 Hz band power for a primary electrode exceeded one standard deviation above the 50-trial mean for each respective electrode, then five immediately adjacent electrodes were analyzed. The goal was to determine if the 45–70 Hz power value from the same trial at adjacent electrodes also exceeded the mean plus one standard deviation. Finally, if three of the five adjacent electrodes had power values that exceeded one standard deviation above the mean, then the suspected trial was rejected from analysis.

For instance, if trial number 4 was suspected of having EMG noise during the

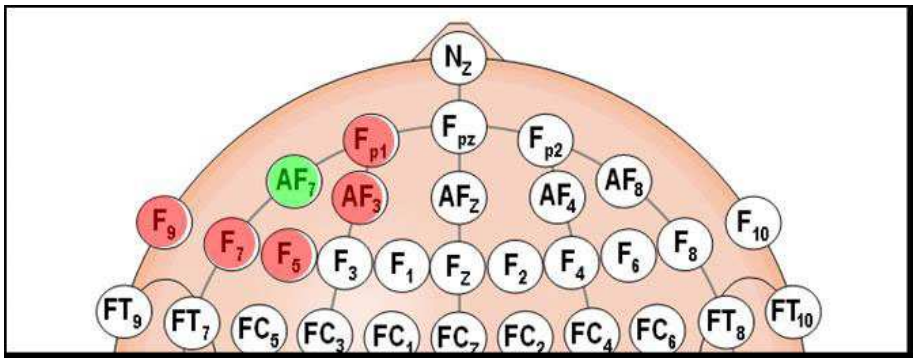

Figure 4.6: If a trial at electrode AF7 was suspected of EMG contamination, then the same trial from 5 neighboring electrodes were also examined.

rest interval at electrode AF7, the same trial were analyzed at electrodes FP1, AF3, F3, F5, and F7, as shown in Fig. 4.6. If three of these five electrodes also exhibited power values for the suspected trial that exceeded one standard deviation above the 50-trial mean for each respective electrode, then trial number 4 was eliminated from analysis.

The decision to use three adjacent electrodes as the decisive criterion was based on the results from an experiment that I conducted. In this experiment, I collected EEG data from a normal adult who performed the experimental motor task 50 times without any intentional frontalis and temporalis muscle contractions, and then 40 times with intentional muscle contractions. Then, a data set of 50 trials was constructed to approximate the same ratio of noisy to clean trials that were visually detected by an expert on the data from our studied subjects. The expert found that approximately 28% (approximately 14 trials) of the 50 total trials of each subject were noisy, so the constructed data set contained 36 EMG-free trials and 14 frontalis and temporalis EMG-contaminated trials, all of which were randomly selected. The constructed data set was then used to test the EMG detection algorithm described above.

I found that the greatest number of EMG-contaminated trials was identified by using the criterion of the data from 3 adjacent electrodes. Six of the 14 contaminated trials were rejected. When four and five adjacent electrodes were used as the criterion,

only 4 of the same 14 contaminated trials were detected. Therefore, the criterion of using data from three adjacent electrodes was chosen.

Mean plus one standard deviation was selected as the optimal threshold in the algorithm because I found that rejecting trials outside this threshold preserved roughly 85%of uncontaminated data, 20% of frontalis contaminated data, and 0% of frontalis and temporalis contaminated data. This threshold was chosen because of its superior performance compared to other threshold values that were evaluated.

4.4.4 ERD Data Processing

Event-related desynchronization in the alpha band mu waves was analyzed using Matlab and Compumedics NeuroScan Edit 4.3.1 using procedures consistent with existing literature [9]. First, the electrode with greatest alpha band pre-movement activity was identified. Subsequently, the frequency component in the alpha band with the greatest change in amplitude was identified as the mu frequency. Next, the data were bandpass filtered at the mu frequency $\pm$ 1 Hz, all the accepted trials of data were averaged, and the ERD percentage value was calculated for each sample of data. Analysis of variance (ANOVA) models were then analyzed to make the following comparisons according to the greatest amount of ERD: stroke versus control and dominant versus non-dominant arm. Peak ERD was analyzed because the percentage of ERD reflects the level of cortical activity [9].

The electrode with the greatest pre-movement planning activity was identified by comparing the average power of a subject's cortical rest (baseline) state to their planning (active) state for the alpha band. For control subjects, the motor planning state was defined as the period two seconds preceding movement onset while the rest state was a two second interval that began five seconds before the active interval. These time periods were selected in light of findings that ERD and MRCP share common timing features [14] and that the mean sensorimotor MRCP onset time for

the control subjects used in this study occurred 1.466 ± 779 ms (roughly 2 s) before movement onset [20]. For the stroke survivors in this study, however, Daly, *et al.* found that the average sensorimotor MRCP start time (2.734 ± 1.205 ms) varied much more than that of the control subjects. In light of this fact, the active state for stroke subjects was defined as the time between the start of the MRCP and movement onset [20]. This definition was based on actual EEG data and for this reason, was potentially more accurate than the approximation methods used by others [6]. The rest interval was chosen as an interval equal in length to the active interval and ended 3 s before the start of the active interval, as seen in Fig. 4.7.

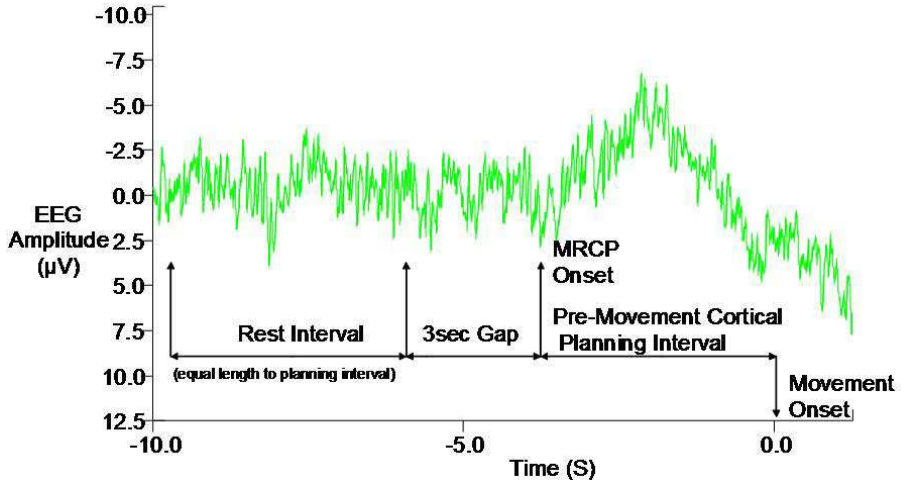

Figure 4.7: Illustration of the cognitive rest and planning intervals identified for stroke subjects.

Matlab's `periodogram.m` function was used to compute the power spectral density (PSD) in the alpha band (8–12 Hz). The `periodogram` function uses the equation

$$Power_{8-12Hz} = \frac{1}{N^2} \sum_{k=\frac{8N}{f_s}}^{\frac{12N}{f_s}} (|X(k)|^2 + |X(N-k)|^2) \tag{4.3}$$

where N is the total number of samples in the rest or planning state and *X(k)* is the kth FFT coefficient, and f_s is the sampling frequency, which was 1000 Hz in this study. The PSD for each of the 50 trials was computed and then averaged for each

subject. The level of activity at an electrode was computed by subtracting the rest PSD from the active PSD and integrating the differences for the 8–12 Hz frequency band. Fig. 4.8 shows an example of the difference between the PSD of the motor planning and rest states. The electrode with the greatest difference in power was identified as the one with peak activity. Electrodes over the sensorimotor frontal and parietal cortices (FCZ, FC1–6, CZ, C1–6, CPZ, and CP1–6) were all analyzed for peak activity.

Next, the individual frequency component at which activity peaked was identified at the peak electrode locations. This was accomplished by finding the frequency in the alpha band that exhibited the greatest change in amplitude between the cognitive rest and active states. This is illustrated in Fig. 4.8.

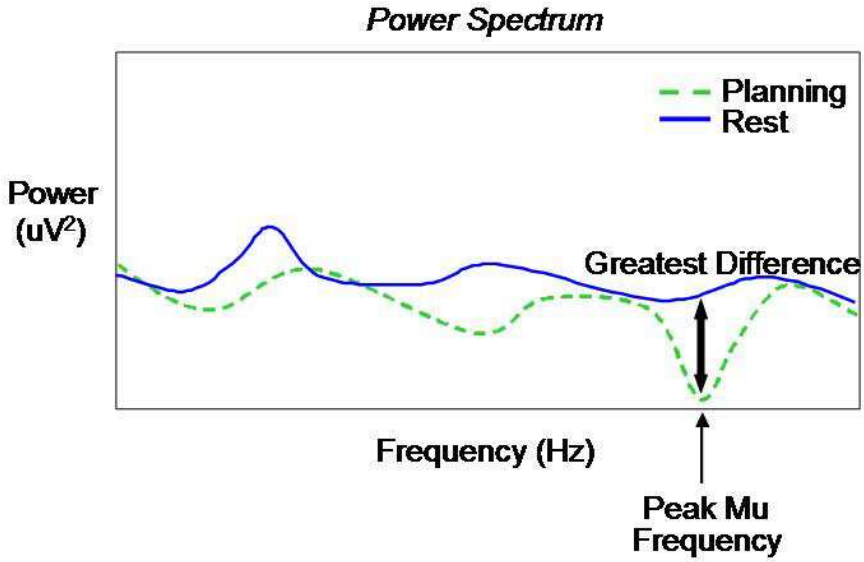

Figure 4.8: The dashed line represents the power spectrum of motor planning state EEG while the solid line represents the power spectrum of rest state EEG. The peak mu frequency was identified at the frequency where there is the greatest difference between the power spectrum values of the two states.

ERD% values were then calculated for the alpha band mu frequency ± 1 Hz using the Event Related Band Power (ERBP) function in NeuroScan Edit 4.3.1. The ERBP function computed ERD percentage using complex demodulation (CD), an

alternative to the classical methods described in the Background section.

Complex demodulation essentially treated the frequency of interest as a carrier wave and preserved only the amplitude variations of that frequency by producing a shifted and filtered version of the original signal centered at the frequency of interest [27]. As an elaboration, it can be assumed a times series signal X_t contains a component x_t that varies in amplitude around a frequency f_0. The signal can be expressed as

$$X_t = x_t + z_t = A_t \cos(f_0 t + \phi_t) + z_t = \frac{A_t}{2}(e^{jf_0 t + \phi_t} + e^{-jf_0 t + \phi_t}) + z_t \tag{4.4}$$

where A_t and ϕ_t are the changes of amplitude and phase of the frequency of interest f_0, and z_t represents all other frequency components in X_t. The first step of the CD algorithm is to multiply X_t by a complex exponential at f_0, which results in

$$Y_t = X_t e^{-jf_0 t} = \frac{A_t}{2} e^{jf_0 t + \phi_t} + \frac{A_t}{2} e^{-jf_0 t + \phi_t} + z_t e^{-jf_0 t} \tag{4.5}$$

The first term on the right hand side of the equation in Fig. 4.5 contains the amplitude and phase variations at the frequency of interest and can be separated from the rest of Y_t by low pass filtering to obtain

$$y_t = \frac{A_t}{2} e^{-jf_0 t + \phi_t} \Rightarrow A_t = 2|y_t| \tag{4.6}$$

Once A_t was computed, a reference interval was identified and the average amplitude over that interval A_{ref} was used in the ERD equation

$$ERD\%_{decrease} = 100 \times \frac{A_{ref} - A_x}{A_{ref}} \tag{4.7}$$

ERD was computed for each sample of data A_x in a trial. Complex demodulation was performed on each trial of data and the data from all trials were averaged together to form one ERD time-series dataset for each subject, as shown in Fig. 4.9. Finally,

because the percentage of ERD correlates to the level of cortical activity, the peak percentage of ERD that occurred within the motor-planning period was recorded and analyzed.

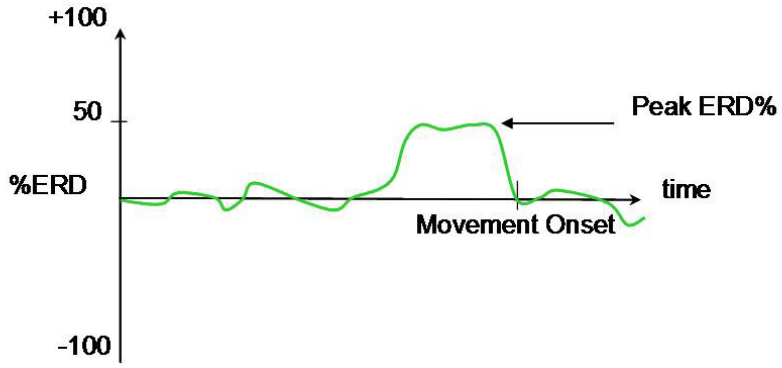

Figure 4.9: Illustration of what a normal adult's ERD% time series plot would look like if they were recorded while performing a movement. The peak ERD% correlates to the greatest amount of cortical activity.

4.4.5 Statistical Analysis

Each subject's maximum percentage of ERD during the motor planning period was recorded and used as the dependent variable for ANOVA. The subjects were grouped into four categories for analysis based on the arm tested: dominant side (right arm tested) control subjects, non-dominant side (left arm tested) control subjects, dominant side stroke survivors, and non-dominant side stroke survivors. Analysis of variance was used to compare stroke to controls and dominant arm to non-dominant arm tested subjects. For comparing stroke versus controls, the independent variable was category (stroke or control) and for comparing handedness, the independent variable was the arm tested.

Chapter 5

Results

The Results section will follow the same order as the ERD signal analysis procedures I described in the methods section. The first section reports the electrode locations where the most pre-movement brain activity occurred. The second section identifies the frequencies at which the greatest brain activity occurred. The third reports the ERD characteristics observed in the subjects.

5.1 Identification of Brain Region With Greatest Activity

5.1.1 Dominant Arm Control Subjects (Right-Arm Tested)

Of the four subjects in this category, all but subject number 4 had the most active electrode on either the working side (odd numbered electrodes) or at medial locations of the brain (CZ and CPZ) (5.1). It is unknown why subject number 4 did not follow this trend and exhibited the greatest activity on the non-working side of the brain (even numbered electrodes) at electrode C6. Subject numbers 1 and 2 had peak activity at working side CPZ and CP5 electrode locations, respectively, and subject number 8 had peak activity at C5. The peak activity at CP electrodes is expected in

normal adults [9]. C5 is not expected to have peak activity due to motor tasks, but since C5 is on the working side of the brain, it is possible for activity to peak there and subject 8 cannot be considered an outlier.

Table 5.1: Right Arm Tested Control Subjects

Subject	Peak Electrode	Alpha Band Power Difference (uV^2)
1.	CPZ	2.75
2.	CP5	2.17
4.	C6	3.08
8.	C5	4.05

Table 5.2: Left Arm Tested Control Subjects

Subject	Peak Electrode	Alpha Band Power Difference (uV^2)
3.	CP2	104.70
6.	FC5	5.20
7.	CP6	26.22

These tables report the control subject electrode locations with the greatest difference in alpha band power for the rest versus motor-planning intervals and the difference values for subjects tested with their dominant (right) arm (Table 5.1) and non-dominant (left) arm (Table 5.2).

5.1.2 Non-dominant Arm Control Subjects (Left-Arm Tested)

There were three subjects in this category. Two of them, subject numbers 3 and 7, had peak activity on the working side at CP2 and CP6, respectively. However, one, subject number 6, had peak activity on the non-working side at FC5 (Table 5.2).

5.1.3 Dominant Arm Stroke Subjects (Right-Arm Tested)

Table 5.3 shows the six post-stroke subjects in this category. Three of them (subject numbers 10, 18, and 19) had the most active electrodes on the non-working side of the brain, while the remaining three showed the most activity on either the working side or center of the brain. The locations of the most active electrodes for all six

subjects were C or FC electrodes. C electrodes were the most active electrodes for three subjects, and FP electrodes were the most active for two subjects.

Table 5.3: Right Arm Tested Stroke Survivors

Subject	Peak Electrode	Alpha Band Power Difference (uV^2)
10.	C6	11.42
12.	FC1	15.29
16.	FC6	3.08
18.	CZ	4.05
19.	C6	5.12
20.	FC5	49.37

Table 5.4: Left Arm Tested Stroke Survivors

Subject	Peak Electrode	Alpha Band Power Difference (uV^2)
9.	CP3	11.17
11.	FC5	1.74
13.	CP5	1.77
14.	FC5	284.45
17.	FC6	7.87

For right-arm tested stroke survivors (Table 5.3) and left-arm tested stroke survivors (Table 5.4), the tables contain the electrode locations with the greatest difference in alpha band power for the rest versus motor-planning intervals and the corresponding difference values.

5.1.4 Non-dominant Arm Stroke Subjects (Left-Arm Tested)

Five subjects were in this category and four of them had the most active electrode on the non-working side. As seen in Table 5.4, subject number 13 was the only one in this group who had the most active C or CP electrode on the working side of the brain. All of the left hand tested stroke subjects showed FC and CP electrodes as the most active; two of them had the most activity at CP electrodes and three at FC electrodes.

5.1.5 Outlier Results

Two of the 20 subjects had unusual results and were therefore excluded from the final analysis. Data from subject numbers 5 (control) and 15 (stroke) were excluded from the analysis due to unusual results observed after comparing the average power of the subjects' rest state against the average power during the motor-planning state. In normal adults, the desynchronization of alpha band EEG waves is expected to occur during the motor-planning state [9]. This can be seen in the EEG data as less alpha frequency band power during the motor-planning state than during the rest state in the alpha and beta frequency bands. Since this phenomenon in the alpha band is utilized to find the electrode with the greatest activity during motor planning (by subtracting the average motor-planning state power from the average rest state power), the resulting value should be a positive number if desynchronization occurred in the motor-planning state and the brain is truly relaxed during the rest state.

Table 5.5: Data from Outliers

Subject	Peak Electrode	Alpha Band Power Difference (uV^2)
5.	CP2	-0.17
15.	FC6	-6.94

Unlike the other subjects, subjects number 5 and 15 had negative alpha band power difference values.

However, none of the electrodes in the data from subject numbers 5 and 15 have positive values. Table 5.5 shows the electrodes for these two subjects with the least negative alpha band power differences. Without a positive difference between rest and motor-planning states, it cannot be concluded that there was activity of the brain during motor planning, nor can a peak mu wave frequency be defined. Hence, these two subjects were excluded.

5.2 Identification of Frequency with Greatest Brain Activity

The mu frequency is defined as the frequency at which there is the greatest difference in rest versus pre-movement power. In normal adults, a mu frequency of around 10 Hz is expected [9].

5.2.1 Dominant Arm Control Subjects (Right-Arm Tested)

As seen in Table 5.6, within the alpha band, the highest mu frequency detected was 10 Hz and the lowest was 8 Hz. The mean mu frequency for this group was 9.13 ($\pm$ 1.3) Hz.

Table 5.6: Right Arm Tested Controls

Subject	Mu Frequency (Hz)
1.	8.5
2.	10.0
4.	8.0
8.	10.0
Mean	9.1
Std. Dev.	1.3

Table 5.7: Left Arm Tested Controls

Subject	Mu Frequency (Hz)
3.	9.0
6.	8.0
7.	10.4
Mean	9.1
Std. Dev.	1.2

Frequencies at which there is greatest pre-motor planning activity for right-arm tested control subjects (Table 5.6) and for left-arm tested control subjects (Table 5.7).

5.2.2 Non-Dominant Arm Control Subjects (Left-Arm Tested)

As seen in Table 5.7, the highest mu frequency detected was 10.4 Hz and the lowest was 8 Hz. The mean mu frequency for this group was also 9.13 (± 1.2) Hz.

5.2.3 Dominant Arm Stroke Survivors (Right-Arm Tested)

From Table 5.8, the highest mu frequency detected was 11.4 Hz and the lowest was 8 Hz. The mean mu frequency for this group was 8.9 (± 1.3) Hz.

Table 5.8: Right Arm Tested Stroke Survivors

Subject	Mu Frequency (Hz)
10.	11.4
12.	8.2
16.	8.0
18.	8.5
19.	9.0
20.	8.5
Mean	8.9
Std. Dev.	1.3

Table 5.9: Left Arm Tested Stroke Survivors

Subject	Mu Frequency (Hz)
9.	11.2
11.	9.5
13.	9.7
14.	8.0
17.	8.2
Mean	9.3
Std. Dev.	1.3

Frequencies at which there is greatest pre-motor planning activity for right-arm tested control subjects (Table 5.8) and for left-arm tested control subjects (Table 5.9).

5.2.4 Non-dominant Arm Stroke Survivors (Left-Arm Tested)

From Table 5.9, the highest mu frequency detected was 11.2 Hz and the lowest was 8 Hz. The mean mu frequency for this group was 9.3 (± 1.3) Hz.

Both control and stroke subjects had average peak mu frequencies of approximately 9 (± 1.3) Hz, which is consistent with normal adults according to literature [9]. Since the individual mu frequencies can vary from 8 to 12 Hz, these results were within the expected norms.

5.3 Peak ERD% at the Mu Frequency

The peak ERD percentage at the mu frequency was determined by examining the times-series ERD data and finding the maximum ERD value in the interval of time between the onset of the MRCP and movement onset. Because the onset of the MRCP reflects the start of motor planning and the timing of ERD and MRCP coincide, the EEG desynchronization occurring in this time interval reflected cortical activity most relevant to motor planning of the motor task [14].

5.3.1 Control Subjects

The mean peak ERD value for right arm tested controls was 59.7 (± 10.5 standard deviation)% and the range was 41.4–71%. For left arm tested controls, the mean peak ERD was 96.7 (± 7.7)% with a range of 81.9–96.7%. These results showed that the ranges of the left and right arm tested controls do not overlap and the ANOVA model of the values in Table 5.10 and 5.11 confirmed that they were significantly different ($p = 0.008$). The difference can be seen in Figure 5.1.

5.3.2 Stroke Survivors

From Table 5.12, right arm tested stroke subjects had a mean peak ERD of 46.4 (± 11)% and a range of 42.8–64.8%. From Table 5.13 shows that left arm tested stroke subjects had a mean peak ERD of 66.4 (± 12.3)% with a range of 52.2–80.1%. ANOVA model analysis revealed a statistically significant difference between the left

Table 5.10: Right Arm Tested Controls

Subject	Peak ERD (%)
1.	72.0
2.	63.6
4.	47.4
8.	55.8
Mean	59.7
Std. Dev.	10.5

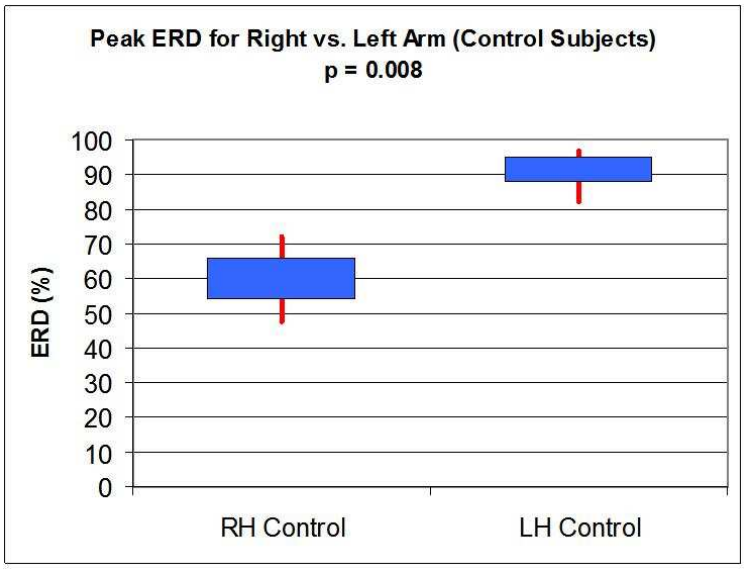

Figure 5.1: Boxplot of peak ERD for control subjects. For each boxplot, the box is centered about the mean, the upper edge of the box represents the 3rd quartile and the lower side represents the 1st quartile. The vertical lines span the range of the data. They were significantly different (p = 0.008).

and right arm tested stroke survivors (p = 0.01). Fig. 5.2 illustrates the difference between these two groups.

Table 5.11: Left Arm Tested Controls

Subject	Peak ERD (%)
3.	96.7
6.	81.9
7.	93.2
Mean	90.6
Std. Dev.	7.7

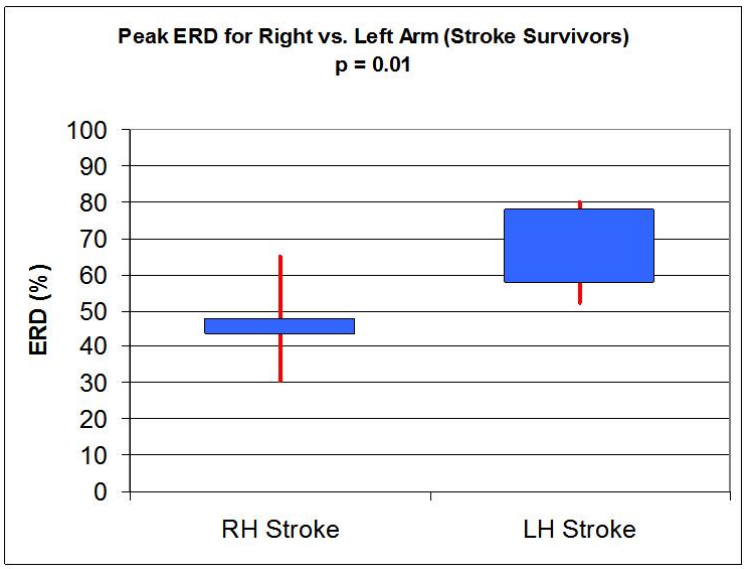

Figure 5.2: Boxplot of peak ERD for stroke survivors. a statistically significant difference between the left and right arm tested stroke survivors (p = 0.01).

5.3.3 Controls vs. Stroke Survivors (Right-Arm Tested)

Next, the right-arm tested controls and right-arm tested stroke survivors were compared. An ANOVA model on the values shown in Table 5.10 and Table 5.12 revealed that the controls and stroke survivors were not significantly different (p = 0.09). However, a statistical power analysis was performed and showed that a significant

difference (alpha = 0.05, $p < 0.05$) could have been detected if there had been a total of 30 dominant arm subjects. Fig. 5.3 illustrates the data for these two groups.

Table 5.12: Right Arm Tested Stroke Survivors

Subject	Peak ERD (%)
10.	45.1
12.	30.6
16.	48.1
18.	47.1
19.	64.8
20.	42.8
Mean	46.4
Std. Dev.	11.0

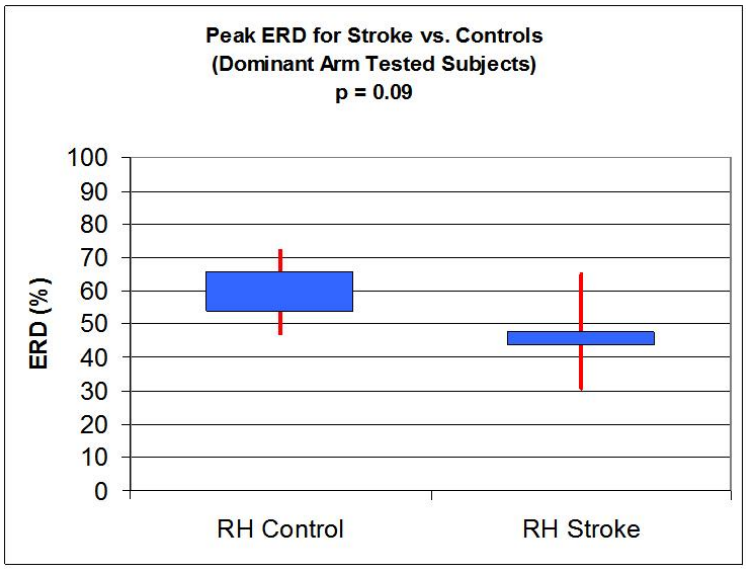

Figure 5.3: Boxplot of peak ERD for right-arm tested subjects. Controls and stroke survivors were not significantly different (p = 0.09).

5.3.4 Controls vs. Stroke Survivors (Left-Arm Tested)

An ANOVA model on the values shown in Table 5.13 and Table 5.11 revealed that the left-arm tested stroke survivors had significantly less peak ERD versus the left-arm tested control subjects (p = 0.023). Fig. 5.4 illustrates the data for these two groups.

Table 5.13: Left Arm Tested Stroke Survivors

Subject	Peak ERD (%)
9.	57.5
11.	52.2
13.	77.8
14.	80.1
17.	64.2
Mean	66.4
Std. Dev.	12.3

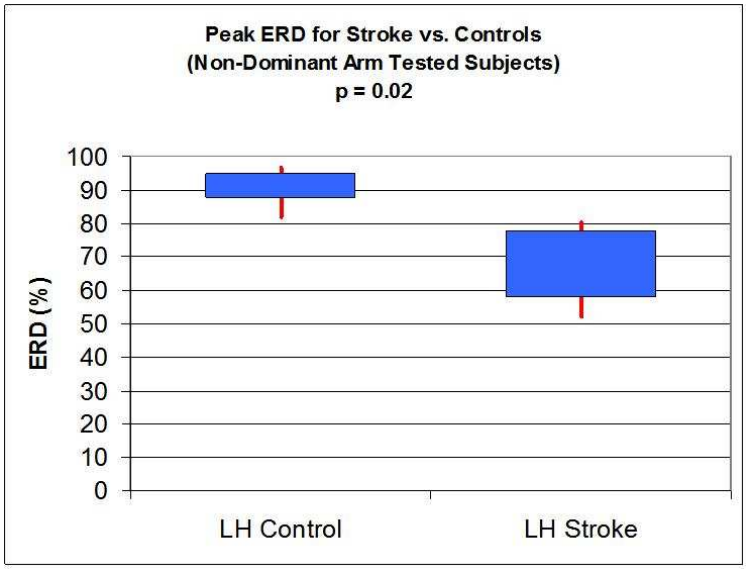

Figure 5.4: Boxplot of peak ERD for left-arm tested subjects. Left-arm tested stroke survivors had significantly less peak ERD versus the left-arm tested control subjects ($p = 0.023$).

5.3.5 All Stroke Survivors vs. All Control Subjects

An ANOVA model was analyzed on a group consisting of all 7 healthy subjects (both left and right-arm tested) and a group consisting of all 11 stroke survivors (both left and right-arm tested). From Table 5.14, the mean peak ERD% for all control subjects was 72.9 ($\pm$ 18.7)% and 55.5 ($\pm$ 15.1) % for all stroke survivors. There was a statistically significant difference between the control and stroke groups ($p = 0.002$). Fig. 5.5 illustrates this difference.

Table 5.14: Comparison of all Subjects by Category

All Control Subjects	All Stroke Survivors
Mean Peak ERD%: 72.9	Mean Peak ERD%: 55.5
Standard Deviation: 18.7	Standard Deviation: 15.1

The peak ERD averages for a group consisting of all the control subjects and a group consisting of all the stroke subjects, regardless of the arm tested.

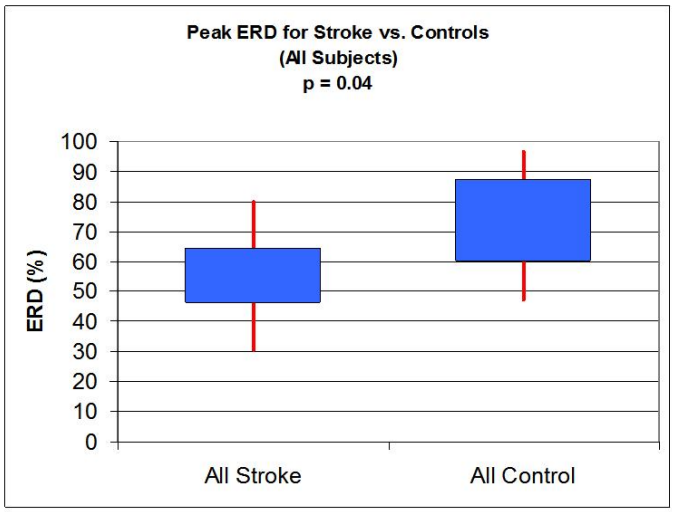

Figure 5.5: Boxplot of peak ERD for right-arm tested subjects. There was a statistically significant difference between the control and stroke groups ($p = 0.002$).

Chapter 6

Discussion

This section reviews the main findings of the study with regard to existing literature, covers the extensions to literature and discusses some limitations of the study. Finally, future study directions are discussed.

6.1 Extensions to Literature

The main findings from this study extend the literature in two ways: first in the effects of handedness on shoulder-elbow movement planning and second, in the effects of stroke on shoulder-elbow movement planning.

There was a statistically significant difference in the peak ERD% of control versus stroke subjects ($p = 0.002$). Also, for both stroke survivors and healthy controls, there was a statistically significant difference in the peak ERD% between those who used their dominant versus non-dominant arms ($p = 0.008$ for controls and $p = 0.02$ for stroke survivors).

This finding extended the literature regarding the effects of hand dominance on pre-movement brain activity. These results are consistent with the findings of others who studied finger motions in healthy controls. Prior studies showed that there was more pre-movement cortical activity in healthy adults for non-dominant hand finger

movements versus the dominant hand [13], [24], and [21]. Specifically, Stancak [24] and Bai [21] both found that ERD occured at significantly higher percentages for healthy adults moving fingers on the non-dominant hand versus the dominant hand.

In the current study, the effect of hand dominance on ERD% during shoulder-elbow movement was consistent with literature for both control and stroke subjects on finger movements, showing significantly higher peak ERD% when the non-dominant arm was tested versus the dominant arm ($p < 0.05$). This observation showed that handedness significantly influenced pre-movement brain activity for arm motion in stroke survivors and highlights hand-dominance as an important dependent variable in the design of future experiments on stroke survivors.

6.2 Limitations

This study was limited by noise and EEG data acquisition methods. Even though measures were taken to electrically isolate the EEG recording system, the data from all subjects in this study was affected by an unknown noise source that introduced signals ranging from 19–21 Hz into all channels of the EEG data record. This noise prevented the accurate analysis of beta frequency mu waves, which are also known to reflect pre-movement cortical activity.

Also, no eye blink detection electrodes were used for the data collections so blink contaminated data was rejected by visual inspection. Finally, the detection of facial and scalp muscle EMG contamination of the EEG data was made difficult because all EEG data beyond 40 Hz was filtered out by the amplifier settings. EMG in the scalp and facial muscles can peak anywhere in the range of 45–70 Hz, so it would be most beneficial for EMG detection if frequencies below 70 Hz are not filter out.

6.3 Conclusion

The peak ERD% of stroke survivors was significantly lower than that of healthy subjects. Also, subjects who used the non-dominant arm had significantly greater ERD% than those who used their dominant arm.

6.4 Future Work

Because of the limitations of this study, the beta band component of mu waves could not be studied, but it is known to exhibit ERD during pre-motor cortical planning in the hand movements of healthy adults and in stroke survivors [9], [8]. Therefore, an investigation into the behavior of beta band mu wave pre-movement ERD is one area of future study. In addition to mu waves, high-frequency EEG waves are also known to reflect cortical activity, but have yet to be studied in stroke survivors. A study on monkeys by Heldman has reported that waves of frequencies ranging from 31–200 Hz (high frequency waves) contained signal characteristics that can be used to predict arm velocities during a circle drawing task (high frequency waves were not studied in this thesis because amplifier filters were set to cutoff frequencies above 40 Hz) [28] . Heldman's study used intracortical electrodes, which have much higher frequency resolution than scalp-mounted electrodes, but scalp electrodes are routinely used to study frequencies up to 100 Hz and even higher-frequency recordings are recommended by the emerging Full-band EEG (FbEEG) recording standard [9], [29]. Investigations of high-frequency EEG characteristics in stroke survivors do not exist in literature, but this is an area of future study that can potentially provide important findings.

Also, by virtue of the experimental paradigm, our study did not produce measures directly comparable to conventional BCI measures (which correlate brain rhythm control to target accuracy). Therefore, additional work needs to be performed to

directly relate the current study to BCI applications.

Bibliography

[1] Interactive Motion Technologies Inc., "Interactive motion technologies product description pamphlet," Cambridge, MA, 2004.

[2] "Images for Physcology 220," University of Virginia, August 2005. [Online]. Available: http://cti.itc.virginia.edu/ psyc220/

[3] J. Malmivuo and R. Plonsey, *Bioelectromagnetism*, 1st ed. New York, New York: Oxford University Press, 1995.

[4] G. Pfurtshceller and L. H. Lopes da Silva, "Event-related EEG/MEG synchronization and desynchronization: basic principles," *Clinical Neurophysiology*, vol. 110, pp. 1842–1857, November 1999.

[5] Compumedics Neuroscan Inc., "Compumedics neuroscan synamps brochure," 2005.

[6] I. I. Goncharova, D. J. McFarland, T. M. Vaughan, and J. R. Wolpaw, "EMG contamination of EEG: spectral and topographical characteristics," *Clinical Neurophysiology*, vol. 114, pp. 1580–1593, March 2003.

[7] J. Wolpaw, N. Birbaumer, D. J. McFarland, G. Pfurtscheller, and T. M. Vaughan, "Brain-computer interfaces for communication and control," *Clinical Neurophysiology*, vol. 113, pp. 767–791, June 2002.

[8] T. Platz, I. H. Kim, H. Pintschovius, T. Winter, A. Kieselbach, K. Villringer, K. R., and K. Mauritz, "Multimodal EEG analysis in man suggests impairment-specific changes in movement-related electric brain activity after stroke," *Brain*, vol. 123, pp. 2475–2490, December 2000.

[9] E. Niedermeyer and L. H. Lopes da Silva, *Electroencephalography: Basic Principles, Clinical Applications, and Related Fields*, 4th ed. Baltimore, MD: Williams and Wilkins, 1999.

[10] J. Bogousslaysky and L. R. Caplan, *Stroke Syndromes*, 2nd ed. Cambridge, NY: Cambridge University Press, 2001.

[11] A. J. Stancak and G. Pfurtscheller, "Event-related desynchronisation of central beta-rhythms during brisk and slow self-paced finger movements of dominant

and nondominant hand," *Brain Research: Cognitive Brain Research*, vol. 4, pp. 171–183, October 1996.

[12] W. S. Newman, November 2005, personal communication.

[13] I. M. Tarkka and M. Hallet, "Cortical topography of premotor and motor potentials preceding self-paced, voluntary movement of dominant and non-dominant hands," *Electroencephalography and Clinical Neurophysiology*, vol. 75, pp. 36–43, February 1990.

[14] C. Toro, G. Deuschl, R. Thatcher, S. Sato, C. Kufta, and M. Hallet, "Event-related desynchronization and movement-related cortical potentials on the ECoG and EEG," *Electroencephalography and Clinical Neurophysiology*, vol. 93, pp. 380–389, October 1994.

[15] J. Wolpaw, D. J. McFarland, G. W. Neat, and C. A. Forneris, "An EEG-based brain-computer interface for cursor control," *Electroencephalography and Clinical Neurophysiology*, vol. 78, pp. 252–259, March 1991.

[16] J. Wolpaw and D. J. McFarland, "Control of a two-dimensional movement signal by a noninvasive brain-computer interface in humans," *Proceedings of the National Academy of Sciences*, vol. 101, pp. 17 849–17 854, December 2004.

[17] L. Sterns, P. Asselman, A. Pogosyan, C. Loukas, A. J. Thompson, and P. Brown, "Corticocortical coupling in chronic stroke: its relevance to recovery," *Electroencephalography and Clinical Neurophysiology*, vol. 63, pp. 475–484, August 2004.

[18] R. Riener, T. Nef, and G. Colombo, "Robot-aided neurorehabilitation of the upper extremities," *Medical and Biological Engineering and Computing*, vol. 43, pp. 2–10, January 2005.

[19] P. S. Lum, C. G. Burgar, P. C. Shore, M. Majmundar, and M. Van der Loos, "Robot-assisted movement training compared with conventional therapy techniques for the rehabilitation of upper-limb motor function after stroke," *Archives of Physical Medicine and Rehabilitation*, vol. 83, pp. 952–959, June 2002.

[20] J. J. Daly, Y. Fang, E. M. Perepezko, V. Siemionow, and G. Yue, "Prolonged cognitive planning time, elevated cognitive effort, and relationship to coordination and motor control following stroke," 2004, abstract submitted for review.

[21] O. Bai, Z. Mari, S. Vorbach, and M. Hallett, "Asymmetric spatiotemporal patterns of event-related desynchronization preceding voluntary sequential finger movements: a high-resolution eeg study," *Clinical Neurophysiology*, vol. 116, pp. 1213–1221, March 2005.

[22] E. Labyt, W. Szurhaj, J.-L. Bourriez, F. Cassim, L. Defebvre, A. Destee, J. D. Guieu, and P. Derambure, "Changes in oscillatory cortical activity related to a visuomotor task in young and elderly healthy subjects," *Clinical Neurophysiology*, vol. 114, pp. 1580–1593, March 2003.

[23] G. R. Muller-Putz, R. Scherer, G. Pfurtscheller, and R. Rupp, "EEG-based neuroprosthesis control: a step towards clinical practice," *Neuroscience Letters*, vol. 382, pp. 169–174, April 2005.

[24] A. J. Stancak and G. Pfurtscheller, "The effects of handedness and type of movement on the contralateral preponderance of mu-rhythm desynchronisation," *Electroencephalography and Clinical Neurophysiology*, vol. 99, pp. 174–182, August 1996.

[25] H. H. Jasper, "Report of the committee on methods of clinical examination in electroencephalography," *Electroencephalography and Clinical Neurophysiology.*, vol. 10, pp. 370–375, 1958.

[26] D. J. McFarland, L. M. McCane, S. V. David, and J. R. Wolpaw, "Spatial filter selection for EEG-based communication," *Electroencephalography and Clinical Neurophysiology.*, vol. 103, pp. 386–394, September 1997.

[27] R. Draganova and D. Popivanov, "Assessment of EEG frequency dynamics using complex demodulation." *Physiological Research*, vol. 48, pp. 157–165, Setptember 1999.

[28] D. A. heldman, W. Wang, S. S. Chan, and D. W. Moran, "Local field potential spectral tuning in motor cortex during reaching and drawing movements," Society for Neuroscience Abstracts, October 2004, presented in San Diego, CA October 23-27.

[29] S. Vanhatalo, J. Voipio, and K. Kaila, "Full-band EEG (FbEEG): an emerging standard in electroencephalography," *Clinical Neurophysiology*, vol. 116, pp. 1–8, January 2004.